BRAND: Ultra-Wideband Feed Development for the European VLBI Network - A Dielectrically Loaded Decade Bandwidth Quad-Ridge Flared

BRAND: Ultra-Wideband Feed Development for the European VLBI Network - A Dielectrically Loaded Decade Bandwidth Quad-Ridge Flared Horn

Jonas Flygare[1], Miroslav Pantaleev[1], Simon Olvhammar[1]
[1](Onsala Space Observatory): Dept. of Space, Earth and Environment, Chalmers University of Technology, SE-41296-Gothenburg, Sweden, jonas.flygare@chalmers.se

***Abstract*—We present the design of an ultra-wideband dielectrically loaded Quad-Ridge Flared Horn (QRFH) feed for the European Very Long Baseline Interferometry Network (EVN) developed under the RadioNet project BRoad-bAND (BRAND). The feed covers a frequency bandwidth ratio of 10:1 and has an average aperture efficiency of 50 percent simulated in primary focus setup on the Effelsberg telescope (f/D = 0.3). The feed is dual-polarized and has an input reflection better than -10 dB over the whole 1.5-15.5 GHz frequency band. We also introduce an Analytic-Spline-Hybrid (ASH) optimization scheme for the QRFH ridge and sidewall profiles.**

***Index Terms*—wideband, feed, quad-ridge flared horn, dielectric load, optimization, radio astronomy**

I. Introduction

The European Very Long Baseline Interferometry Network (EVN) is a network of radio telescopes for astronomy located around the globe that produces high resolution observations of astronomical sources. The frequency bands L-, S-, C-, and X-band ($1.6 - 8.4$ GHz) are available across the entire EVN, through dedicated receivers, with some stations providing even higher and lower frequencies. In astronomical Very Long Baseline Interferometry (VLBI) the development of ultra wideband receivers give possibilities to cover a large number of frequency sub-bands for simultaneous observations. The BRoad-bAND (BRAND) project is the vision to create a receiver system that is easy adaptable across this entire network, with a front-end covering $1.5 - 15.5$ GHz (10:1) with a single feed [1]. This would allow for spectroscopy of different astronomical masers over the frequency bands simultaneously, variations of polarised emission to identify the properties of astronomical objects and significantly improve the ultraviolet imaging. A second advantage of the broad frequency band is the compatibility with the VLBI Global Observing System (VGOS) that covers the $2 - 14$ GHz frequency range. This is used for geodetic VLBI which determines geodetic and geodynamic parameters with high precision [2].

We present the design and development of a dielectrically loaded ultra-wideband Quad-Ridge Flared Horn (QRFH) covering the BRAND frequency band, $1.5 - 15.5$ GHz. The feed is optimized for the wide subtended angle of the Effelsberg telescope's primary focus ($2 \times 79°$) which is a key station in the EVN. The emphasis in the paper is put on the optimization of the feed profile, combining the analytic and spline profile and the effect of the dielectric load centered in the feed.

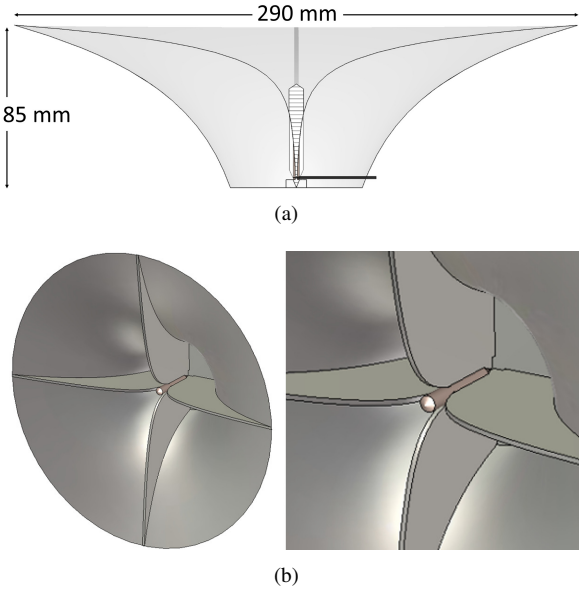

Fig. 1. Quad-Ridge Flared Horn (QRFH) illustrated in (a) cross-section and (b) perspective view with zoom-in on the dielectric load at the center.

II. Specifications for BRAND

One of the goals for the BRAND project is to make the decade bandwidth receiver system adaptable to all the EVN telescope geometries, which ranges in focal length over dish diameter ratio (f/D) from 0.3 to above 2.5. For the first demonstration of concept the axially-symmetric Effelsberg 100 m telescope will be the geometry used with the feed mounted in primary focus. The focal length is $f = 30$ m which gives $f/D = 0.3$ and a half-subtended angle of $\theta_0 = 79°$, illustrated in Fig. 3(a). The decade frequency band of $1.5 - 15.5$ GHz together with the wide subtended angle requires a careful optimization procedure that keeps the feed dimensions within reasonable limits for manufacturing. The specifications mentioned puts emphasis on a highly optimizable feed design.

III. Quad-Ridge Flared Horn

During the last couple of decades many different feeds for radio astronomy have been successfully developed. The QRFH have inherent high radiation efficiency due to mostly metal structure and can give near-constant beamwidth over large bandwidths [3] – [9]. The average aperture efficiency has been shown to vary from 80 % down to 60 % over bandwidth ratios of 3:1 to 7:1 and half-subtended angles of $\theta_0 = 40°-70°$. In general the input reflection can be optimized to better than -10 dB across the bandwidth. The QRFH offers the possibility of dual coaxial 50 Ω single-ended feeding with one Low-Noise Amplifier (LNA) per polarization as well as balun-free differential quadraxial feeding [6]. The feed is built up by a circular or square horn profile that contains two sets of orthogonal ridges, see Fig. 1, which enables the wideband characteristics and reduces horn dimensions. Traditionally the profiles has been modeled with analytical equations, e.g. exponential and sinusoidal [3] – [6], and more recently through point defined splines [7], [8].

A. Model for Optimization

The ridge and horn sidewall profile used in this design are modeled after exponential functions given in [5], as they have been proven to achieve high aperture efficiency. Each profile consists of five variables and are given according to

$$x_{\mathrm{p}}(z) = A\left(\frac{r_{\mathrm{out}} - r_{\mathrm{in}}}{e^{RL}-1}e^{Rz} + \frac{r_{\mathrm{in}}e^{RL} - r_{\mathrm{out}}}{e^{RL}-1}\right) + (1-A)\left(r_{\mathrm{in}} + (r_{\mathrm{out}} - r_{\mathrm{in}})\frac{z}{L}\right) \quad (1)$$

where r_{in} and r_{out} is the throat and aperture radius respectively. L is defined as the taper length, R is the exponential opening rate and A defines the linear taper in each profile. Two variables are shared between the ridge and sidewall for the flared end-point to coincide. The throat section of the feed is further parametrized in terms of distances between opposite ridges and the distance in the 45° plane for orthogonal ridges. The feed also includes a back-short section and a dielectric load at the center placed between the ridges, which results in a total of 20 individual parameters that constitute the feed model. The feeding of the QRFH consists of two ports with single-ended coaxial feeding pins matched to 50 Ω.

B. Optimization - Stochastic Algorithms

The feed model was designed in CST Microwave Studios which has an internal optimizer providing stochastic optimization algorithms such as Particle Swarm Optimization (PSO) and Genetic Algorithm (GA). CST also provides the possibility to be controlled by MATLAB using VBA programming to implement external optimization routines. Efficiency calculation on the telescope have been calculated using equations for paraboloids defined in [10], with CST asymptotic solver and GRASP Physical Optics (PO). Optimization runs of $1500-5000$ iterations were performed with different setups for parameter search space, algorithm swarm or population size and weighting in the fitness (goal) function. The four main goals shown in Table I, were used in the fitness function for the majority of the optimization, where full beamwidth is denoted BW. The goals were weighted differently, with the most successful combination being the top two goals having double the priority of the bottom two. The span of approximately $\pm 5°$ in the goal function for the E-plane ($\phi = 0°$) 12 dB half-beamwidth, was the most effective to avoid local minimum during the optimization. Attention was put into finding a reasonable frequency resolution for beamwidth evaluation over such a wide band. A fine frequency step would increase the iteration time significantly and the number of frequency points used were in the range of $15 - 29$.

TABLE I
Goals for the fitness function used in optimization

$S11 < -10$ dB
$\mathrm{BW}_{\phi=0°}(12\ \mathrm{dB}) > 2 \times 75°$
$\mathrm{BW}_{\phi=0°}(12\ \mathrm{dB}) < 2 \times 85°$
$\mathrm{BW}_{\phi=90°}(12\ \mathrm{dB}) > 2 \times 50°$

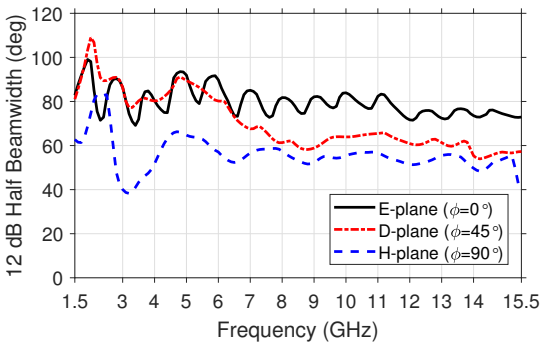

Fig. 2. Simulated 12 dB half-beamwidth for E-plane ($\phi = 0°$), D-plane ($\phi = 45°$), and H-plane ($\phi = 90°$)

IV. Feed Performance

The optimized QRFH design measures 290 mm in aperture diameter and 85 mm in length showing a large flare angle at the edge towards the reflector, see Fig. 1. The E-plane 12 dB half-beamwidth varies with ±5 % around the desired value of 79° for most of the band as seen in Fig. 2. The difference between E- and H-plane is ≈ 20° except at the lower end where a larger deviation occurs. Simulated on the telescope the aperture efficiency η_{a} averages to 50 % over the band, see Fig. 3(b). At the low end of the band, there is clear over illumination of the dish which decreases the spill-over efficiency η_{sp} below 90 %. However, for the majority of the band $\eta_{\mathrm{sp}} > 95$ % which is significantly important for a primary-fed reflector system with the feed facing down towards the ground that has an equivalent noise temperature of 300 K. The polarization efficiency η_{pol} drops below 80 % around $2 - 3$ GHz which results in a lower aperture efficiency. This is a problem that have been shown to occur for analytical profiles, with a suggested solution of instead

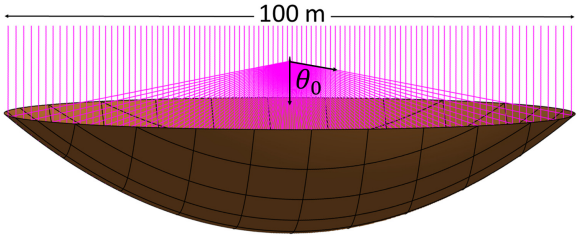

(a)

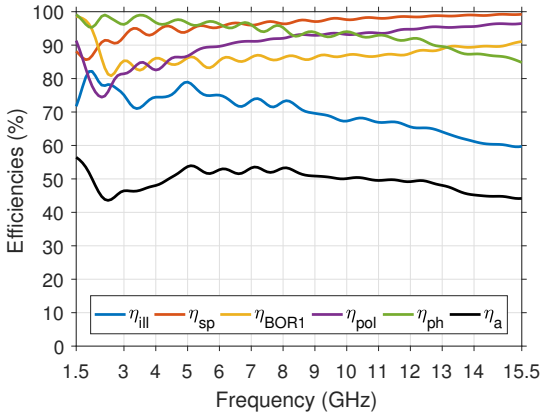

(b)

Fig. 3. (a) Illustration of the wide subtended angle, $2 \times 79°$, of the Effelsberg primary focus ($f/D = 0.3$). (b) Efficiencies for the QRFH simulated in the Effelsberg geometry. Efficiencies - η_{ill}: illumination, η_{sp}: spill-over, η_{BOR1}: BOR1, η_{pol}: polarization, η_{ph}: phase, η_a: aperture.

using spline profiles [8]. We will address a combined approach to analytic and spline profiles in section V to potentially improve efficiencies in future designs. In Fig. 5 the simulated E-, D-, and H-plane are shown in co-polarization (solid lines) and cross-polarization (dashed lines) with the dash-dotted box representing the 12 dB taper at $2 \times 79°$ beamwidth. The cross-polarization level in D-plane explains why the η_{pol} drop is so significant for low frequencies. It has previously been shown that introduction of a dielectric load into the QRFH can improve the beam pattern, especially at the high end of the band [9]. A Polytetrafluoroethylene (PTFE) dielectric rod ($\epsilon_r \approx 2.1$) is inserted at the center of the feed between the ridges, as seen in Fig. 1. This improves the illumination efficiency η_{ill} with $5 - 15$ % at the mid and high end of the band, see Fig. 6, as well as a 5 % improvement of the phase efficiency η_{ph}. Dielectric losses introduced by the rod is expected to be small with a physical feed temperature of 20 K inside a cryostat.

The QRFH is excited with two orthogonal coaxial 50 Ω feed pins. Simulated input reflection is below -10 dB for the entire band, see in Fig. 4. We see that the isolation between ports is worse at the high end of the band, and is an effect from the dielectric load. The two ports are separated in physical distance between each other which results in slightly different input reflections. In terms of mode excitation the feed

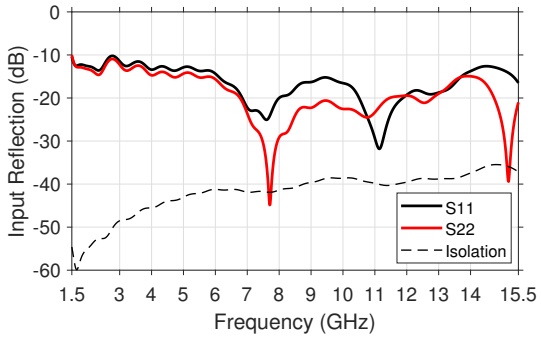

Fig. 4. Input reflection coefficient for the QRFH with 50 Ω single-ended coaxial feeding for dual polarization.

performance could be improved by introducing differential feeding as suggested in [6].

To estimate the sensitivity or System Equivalent Flux Density ($SEFD$) we use a simplified approach to find the antenna noise temperature T_a and system noise temperature T_{sys}. For the primary-fed paraboloid we have

$$\begin{aligned} T_a &= \eta_{sp} T_{sky} + (1 - \eta_{sp}) T_g \\ T_{sys} &= \eta_{rad} T_a + (1 - \eta_{rad}) T_{phy} + T_{rec} \end{aligned} \tag{2}$$

where η_{sp} is the spill-over efficiency, η_{rad} the antenna radiation efficiency. The noise temperature contributions are $\eta_{sp} T_{sky} = T_{mb}$ from the main beam and $(1 - \eta_{sp}) T_g = T_{sp}$ from the ground spill-over. T_{phy} is the physical temperature of the antenna and the equivalent noise temperatures for the sky, ground and receiver are T_{sky}, T_g and T_{rec} respectively. In this model we assume that all spill-over noise contribution T_{sp} comes from the 300 K ground, and the rest of the antenna noise comes from the telescope main beam T_{mb} on sky. The effective area A_{eff} and $SEFD$ is calculated as

$$\begin{aligned} A_{eff} &= \eta_{rad} \eta_a A_{phy} \\ SEFD &= 2 k_B (T_{sys} / A_{eff}) \end{aligned} \tag{3}$$

where A_{phy} is the reflector area, η_a aperture efficiency and k_B is the Boltzmann constant. In Fig. 7(b) the $SEFD$ for different elevations of the sky is shown, where $|\theta| = 90°$ represents zenith. The model is simplified since we assume that all the spill-over is terminated on ground (worst case), which is not the case for lower elevations. However, the dominant effect on lower elevations is the increase in main beam noise due to the atmosphere layer being effectively "thicker" to penetrate at an angle. We also assume uniform noise distribution for the T_{mb} which is also a simplification. At the lower end of the band, the spill-over to ground ($T_g = 300$ K) is dominating the T_{sys} shown in Fig. 7(a) due to the drop in η_{sp}, see Fig. 3(b). Current LNAs can achieve $T_{rec} \approx 5$ K which once again puts emphasis on the spill-over efficiency of the feed. In Fig. 7 we assume $T_{rec} = 7$ K to account for additional noise from back-end and cables.

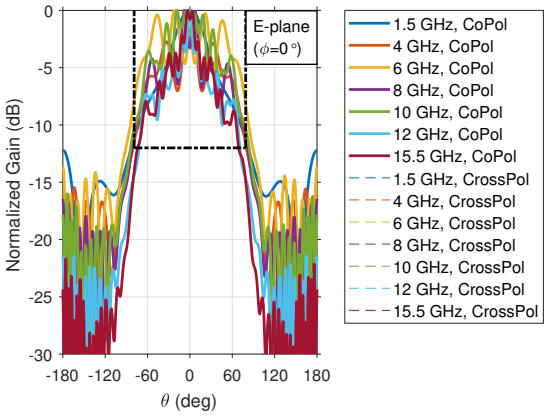

(a)

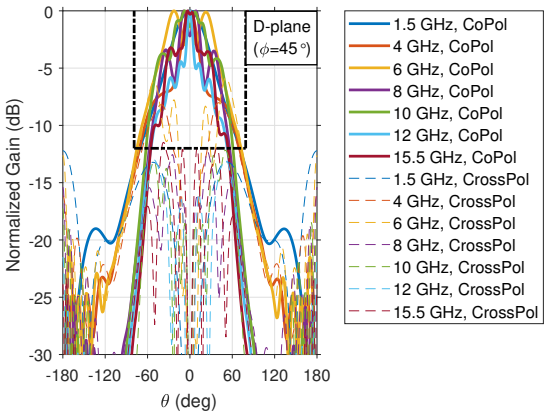

(b)

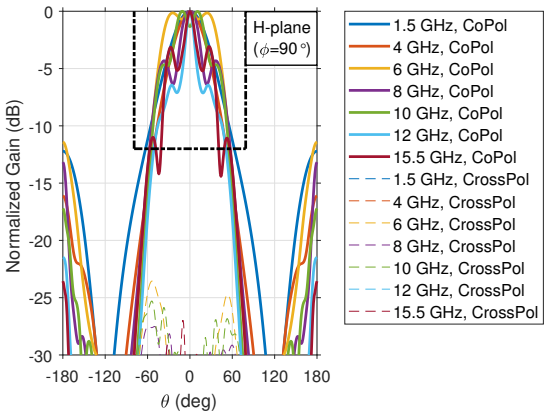

(c)

Fig. 5. Simulated beam patterns, co and cross polarization in Ludwig-3 for (a) E-plane ($\phi = 0°$) (b) D-plane ($\phi = 45°$) (c) H-plane ($\phi = 90°$). The dash-dotted black box represents the 12 dB taper for $2 \times 79°$ beamwidth.

V. Two-Step Optimization - Analytic-Spline-Hybrid (ASH)

This approach combines the use of analytically and spline defined profiles in the attempt to maximize the performance

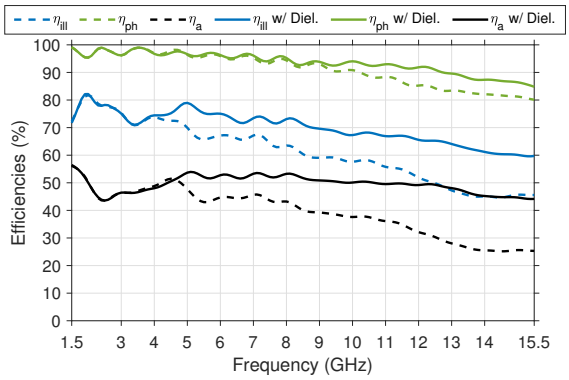

Fig. 6. The effect of dielectrically loading the QRFH shown with efficiencies in the Effelsberg geometry. Efficiencies - η_{ill}: Illumination, η_{ph}: phase, η_a: aperture. Solid lines are with a dielectric load, dashed lines are without.

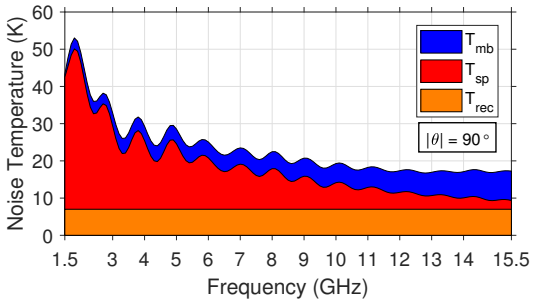

(a)

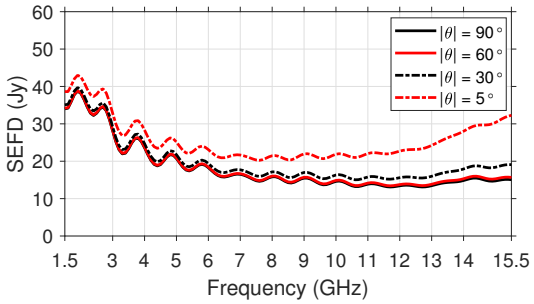

(b)

Fig. 7. (a) Estimated system noise temperature, in zenith direction, with contributions from T_{mb}: main beam, T_{sp}: spill-over, T_{rec}: receiver (b) Estimated $SEFD$ over different elevations.

over a wide frequency band. The analytical QRFH profiles demands less iterations due to the relatively small amount of parameters needed and the splined profiles can be controlled to create more specific details. We combine the two approaches in the Analytic-Spline-Hybrid (ASH) optimization shown with a schematic overview in Fig. 8(a). The general approach is to maximize performance of the analytic model - exponential, sinusoid, tangential and transfer the optimized profile to a spline-defined parametrized copy. This model is then optimized further with different options - full or part of profile, both ridge and sidewall or separate and different

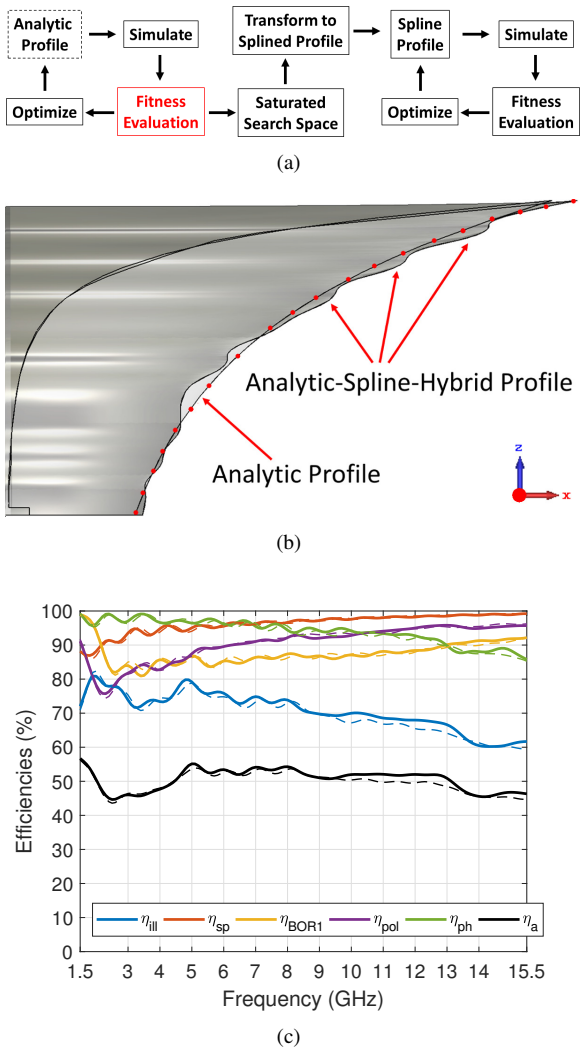

Fig. 8. Analytic-Spline-Hybrid (ASH) optimization (a) flowchart, dashed box (top left) defines the starting point, the red box defines the first break point where analytical profile is transformed to splined profile (red dots in illustration). (b) Exemplifies a QRFH profile after ASH optimization of both ridge and horn profile. (c) Resulting efficiencies for optimization of only the ridge profile with 20 point spline, dashed lines are analytical profile, solid lines are after ASH optimization.

number of spline points. Each point in the spline has a X- and Z-coordinate which can be optimized individually. In Fig. 8(b) the illustration of ASH optimization on the QRFH design is shown. We see the result of an ASH optimization (solid lines) off the ridge profile in Fig. 8(c) with a slight increase in efficiencies, especially at the high end of the band. In this example we transform the analytic ridge profile to a 20 point spline. The average aperture efficiency is increased with ≈ 1 %, but further development of this strategy could improve the design even more. The goals of the fitness function are shown in Table I, with the spline points search space set to vary ± 10 % around the anchor value (original analytic profile). In the example shown here we only vary the X-coordinate of the spline points for simplicity.

VI. Conclusions

We show the feasibility of a 10:1 QRFH feed for a very large half-subtended angle with an average of 50 % aperture efficiency simulated in the Effelsberg telescope primary focus. The introduction of a dielectric load proves to increase the aperture efficiency by $10-20$ % at the mid and high end of the band. Due to the cryogenic temperatures of the feed, the losses in the dielectric can be assumed small. The feed achieves better than -10 dB input reflection over the entire band. With the Analytic-Spline-Hybrid approach for the QRFH we can potentially improve the ultra-wideband performance further.

Acknowledgment

The project leading to this publication has received funding from the European Union's Horizon 2020 research and innovation programme under grant agreement No 730562 [RadioNet]. The authors would like to thank Prof. Jian Yang from the antenna group at the Signals and Systems department of Chalmers University of Technology for valuable feedback.

References

[1] G. Tuccari, W. Alef, M. Pantaleev, J. Flygare, J.A. López Pérez, J.A. López Fernández, G.Schonderbeek, and L. Bezrukos, "BRAND: A very wide-band receiver for the EVN," in *23rd European Very Long Baseline Interferometry Group for Geodesy and Astrometry (EVGA)*, Gothenburg, Sweden, May 2017, pp. 1–3.

[2] J. Flygare, M. Pantaleev, B. Billade, M. Dahlgren, L. Helldner, and R. Haas, "Sensitivity and antenna noise temperature analysis of the feed system for the Onsala twin telescopes," in *23rd European Very Long Baseline Interferometry Group for Geodesy and Astrometry (EVGA)*, Gothenburg, Sweden, May 2017, pp. 1–5.

[3] A. Akgiray and S. Weinreb, "Ultrawideband square and circular quad-ridge horns with near-constant beamwidth," in *International Conference on Ultra-Wideband (ICUWB)*, Syracuse, NY, USA, September 2012, pp. 518–522.

[4] A. Akgiray, S. Weinreb, and W.A. Imbriale, "The quadruple-ridged flared horn: A flexible, multi-octave reflector feed spanning f/0.3 to f/2.5" in *7th European Conference on Antennas and Propagation (EuCAP)*, Gothenburg, Sweden, April 2013, pp. 768–769.

[5] A. Akgiray, S. Weinreb, W. A. Imbriale, and C. Beaudoin, "Circular quadruple-ridged flared horn achieving near-constant beamwidth over multioctave bandwidth: Design and measurements," *IEEE Transactions on Antennas and Propagation*, vol. 61, no. 3, pp. 1099–1108, March 2013.

[6] T. S. Beukman, M. V. Ivashina, R. Maaskant, P. Meyer, and C. Bencivenni, "A quadraxial feed for ultra-wide bandwidth quadruple-ridged flared horn antennas," in *8th European Conference on Antennas and Propagation (EuCAP)*, The Hague, The Netherlands, April 2014, pp. 3312–3316.

[7] B. Billade, J. Flygare, M. Dahlgren, B. Wästberg, and M. Pantaleev, "A Wide-band Feed System for SKA Band 1 Covering Frequencies From 350 - 1050 MHz," in *10th European Conference on Antennas and Propagation (EuCAP)*, Davos, Switzerland, April 2016, pp. 1–3.

[8] B. Dong, J. Yang, J. Dahlström, J. Flygare, M. Pantaleev, and B. Billade, "Optimization and Realization of Quadruple-ridge Flared Horn with New Spline-defined Profiles as a High-efficiency Feed for Reflectors over 4.6 – 24 GHz" *IEEE Transactions on Antennas and Propagation*, September 2017 (Submitted).

[9] A. Dunning, M. Bowen, M. Bourne, D. Hayman, and S. L. Smith, "An ultra-wideband dielectrically loaded quad-ridged feed horn for radio astronomy," in *Topical Conference on Antennas and Propagation in Wireless Communication (APWC)*, Turin, Italy, September 2015, pp. 787–790.

[10] P.-S. Kildal, "Factorization of the feed efficiency of paraboloids and Cassegrain antennas," *IEEE Transactions on Antennas and Propagation*, vol. 33, no. 8, pp. 903–908, August 1985.